Gene Expression in Tea Plant Leaves and New Shoots Under the Influence of ZnO NPs

In this study, we conducted transcriptomic sequencing on tea plant leaves and buds treated with nano zinc oxide. A total of 65.10 Gb Clean Data was obtained from 9 leaf samples, and 70.66 Gb Clean Data from 9 new shoot samples. The percentage of Q20 bases was above 97.63%, and the percentage of Q30 bases was above 93.57% for all 18 samples, indicating high transcriptome quality suitable for subsequent analysis (Table.S3). Clean Reads were aligned with the reference genome shuchazao_V2_Genome.fas (downloadable at: http://tpia.teaplants.cn/download.html) to obtain positional information on the reference genome or genes and unique sequence characteristics of the sequencing samples.

Differential Gene Expression Analysis

To explore the impact of ZnO NPs on gene expression in tea plants, we screened for differentially expressed genes (DEGs) in leaves and new shoots. The selection criteria for DEGs in this experiment were $|\log2\text{Fold Change}| \geqslant 1$ and FDR (False Discovery Rate) < 0.05. A total of 1771 DEGs were identified between T1L and CKL, with 976 upregulated and 804 downregulated; 2448 DEGs were identified between T2L and CKL, with 1308 upregulated and 1140 downregulated (Fig.12A). Between T1S and CKS, 169 DEGs were identified, with 126 upregulated and 43 downregulated; between T2S and CKS, 88 DEGs were identified, with 69 upregulated and 19 downregulated (Fig.12B). Venn diagrams also show the number of DEGs that are common or unique among treatments (Fig.13). To explore the expression patterns of DEGs in tea plant leaves and new

shoots after ZnO NPs treatment, we normalized the data using Z-score and clustered genes with similar or close expression patterns to infer the function of unknown genes or unknown functions of known genes (Fig.14). Furthermore, to study the expression patterns of genes under ZnO NPs treatment, we first normalized the FPKM of all DEGs using R language and then performed Kmeans clustering analysis. Genes in the same cluster have similar trends under ZnO NPs treatment and may have similar functions. We also conducted K-means clustering analysis, with leaf DEGs divided into 10 clusters (Fig.15A) and new shoot DEGs into 9 clusters (Fig.15B), indicating significant differences in gene expression in tea plant leaves and new shoots under different concentrations of treatment.

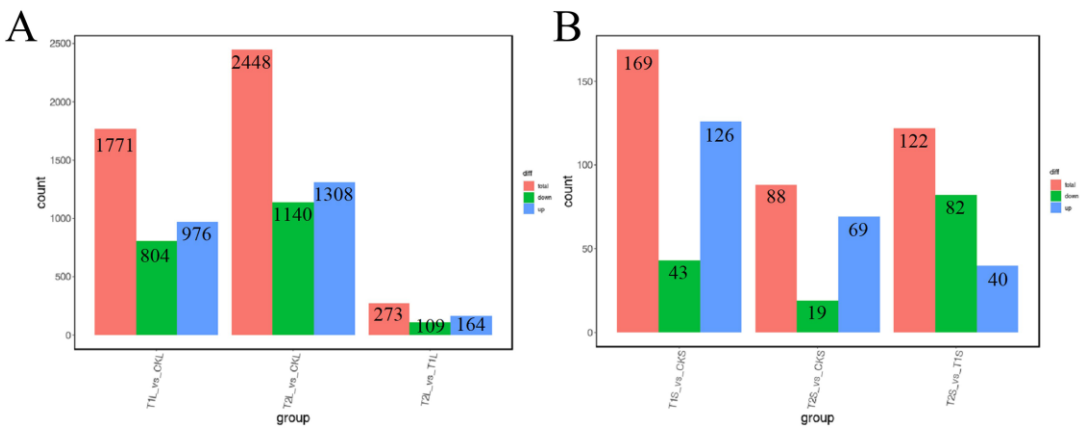

Fig.12 Number of differentially expressed genes in tea plant leaves (A) and new shoots (B) under the influence of ZnO NPs.

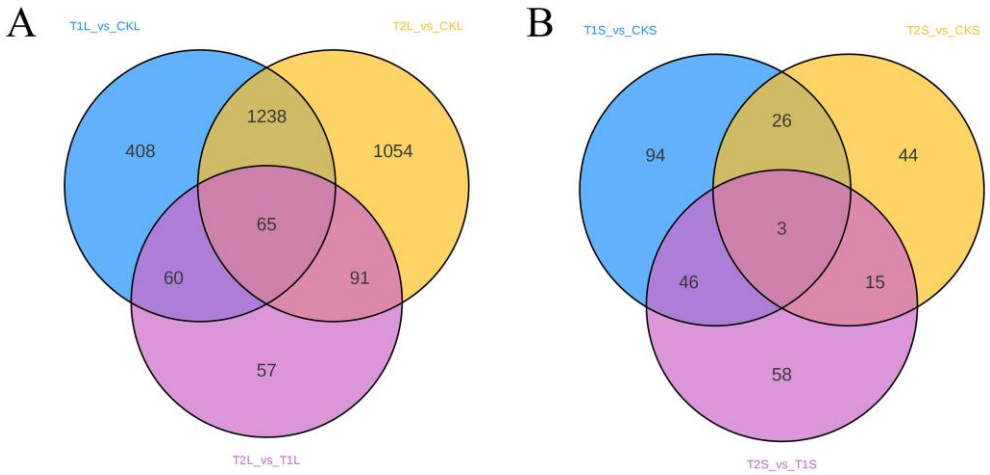

34

35 **Fig.13 Venn diagrams of differentially expressed genes in tea plant leaves (A) and new shoots**

36 **(B) under the influence of ZnO NPs.**

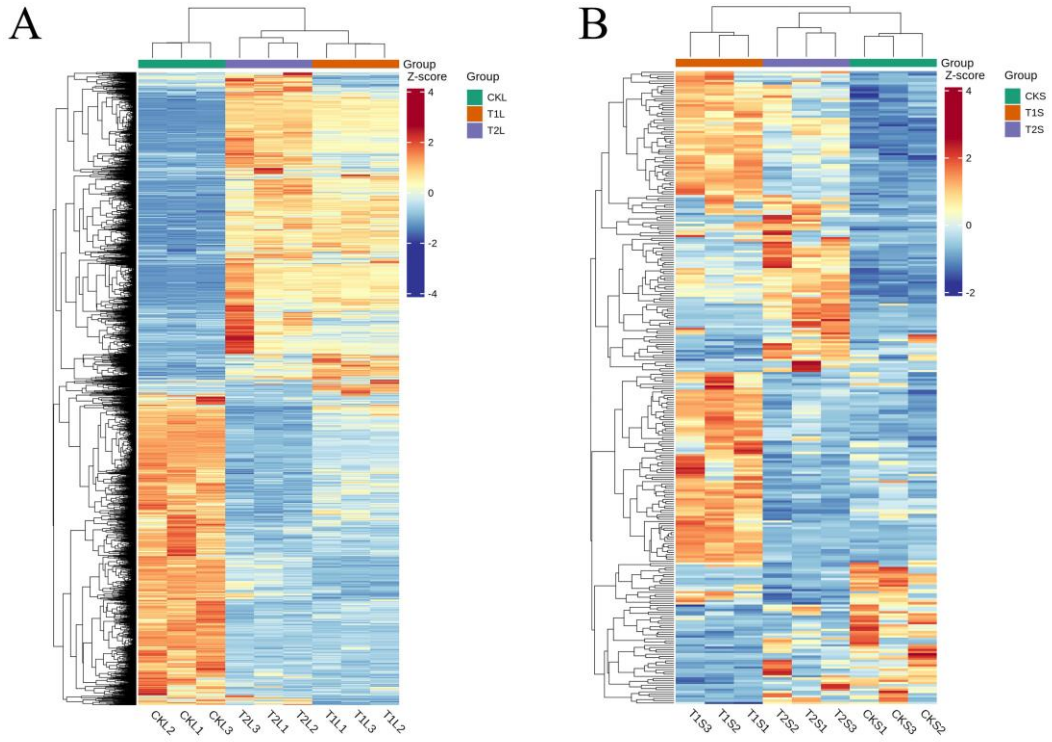

37

38 **Fig.14 Cluster heatmaps of differentially expressed genes in tea plant leaves (A) and new**

39 **shoots (B) under the influence of ZnO NPs.**

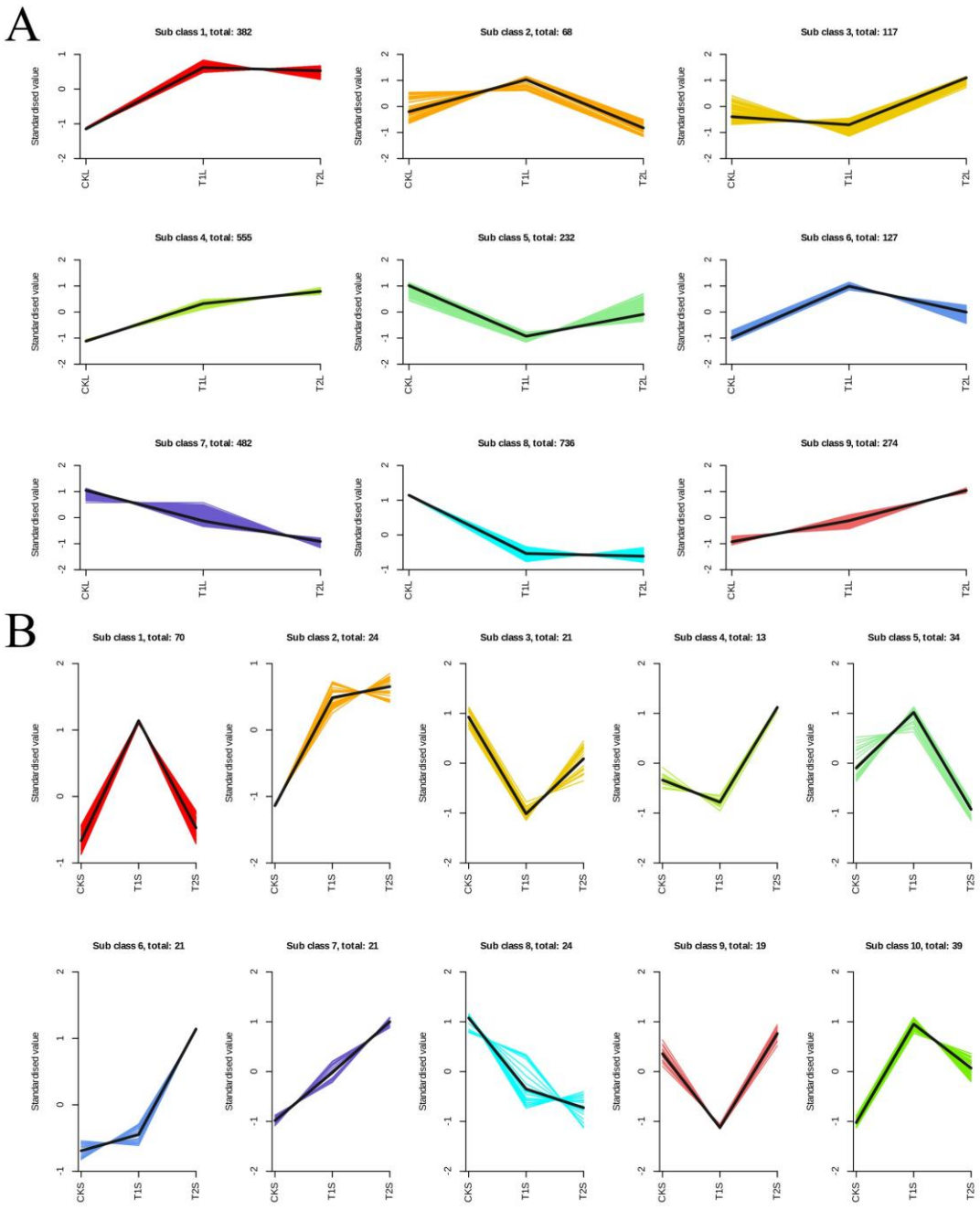

Fig.15 K-means clustering diagrams of differentially expressed genes in tea plant leaves (A) and new shoots (B) under the influence of ZnO NPs.

KEGG Enrichment Analysis of Differentially Expressed Genes

To identify the functions or metabolic pathways enriched by differentially expressed genes and to

elucidate the differences at the gene function and metabolic pathway levels in tea plant leaves and new shoots after ZnO NPs treatment, we performed Kyoto Encyclopedia of Genes and Genomes (KEGG) enrichment analysis on the differentially expressed genes. The results are shown in Fig.16. DEGs between T1L and CKL were mainly enriched in Photosynthesis - antenna proteins (ko00196, Q-value=3.79*10^-10), Biosynthesis of secondary metabolites (ko01110, Q-value=1.37*10^-8), Circadian rhythm – plant (ko04712, Q-value=1.45*10^-8), Metabolic pathways (ko01100, Q-value=2.92*10^-5), alpha-Linolenic acid metabolism (ko00592, Q-value=0.019) and other metabolic pathways (Fig.16A); DEGs between T2L and CKL were mainly enriched in Circadian rhythm - plant (ko04712, Q-value=8.24*10^-12), Biosynthesis of secondary metabolites (ko01110, Q-value=1.22*10^-7), Photosynthesis - antenna proteins (ko00196, Q-value=2.57*10^-7), Metabolic pathways (ko01100, Q-value=0.005), Nitrogen metabolism (ko00910, Q-value=0.007), Starch and sucrose metabolism (ko00500, Q-value=0.020), Biosynthesis of various plant secondary metabolites (ko00999, Q-value=0.025), Plant hormone signal transduction (ko04075, Q-value=0.027), Cutin, suberine and wax biosynthesis (ko00073, Q-value=0.036) and other metabolic pathways (Fig.16B). DEGs between T1S and CKS were mainly enriched in Biosynthesis of secondary metabolites (ko01110, Q-value=1.17*10^-5), Metabolic pathways (ko01100, Q-value=0.013), Ascorbate and aldarate metabolism (ko00053, Q-value=0.031) (Fig.16C); DEGs between T2S and CKS were mainly enriched in Biosynthesis of secondary metabolites (ko01110, Q-value=0.032) (Fig.16D).

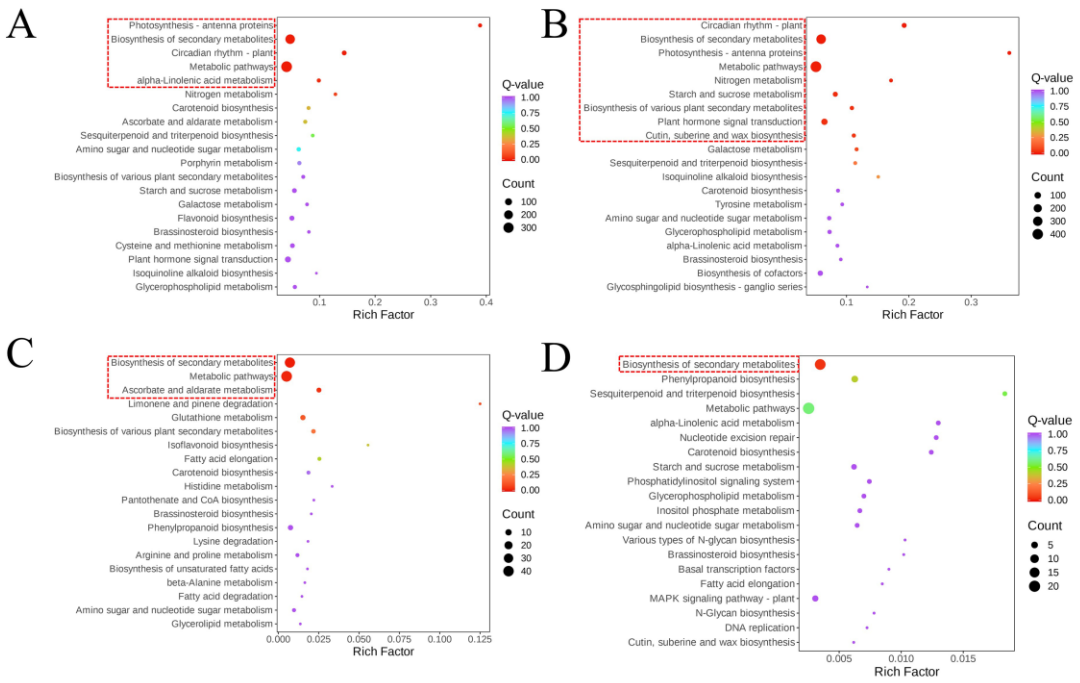

Fig.16 KEGG enrichment pathways of differentially expressed genes in tea plant leaves (AB) and new shoots (CD) under the influence of ZnO NPs. Enrichment analysis between CKL and T1L (A); between CKL and T2L (B); between CKS and T1S (C); between CKS and T2S (D). Pathways within the red dashed box have a Q-value < 0.05, where Q represents the p-value after correction for multiple hypothesis testing.

GO Enrichment Analysis of Differentially Expressed Genes

To explore the roles of differentially expressed genes in molecular function (MF), biological process (BP), and cellular component (CC) in tea plant leaves and new shoots after ZnO NPs treatment, we conducted a Gene Ontology (GO) enrichment analysis at the second hierarchical level. We selected the top 20 most significantly enriched GO terms for presentation, and the results are shown in Fig.17. The differential pathways between T1L and CKL were mainly enriched in isoflavonoid metabolic process, photosynthesis, light harvesting, chlorophyll binding, photosynthesis, light reaction,

response to blue light, photosystem I, and photosynthesis, light harvesting in photosystem I, among others (Fig.17A); between T2L and CKL, the differential pathways were mainly enriched in isoflavonoid biosynthetic process, secondary metabolite biosynthetic process, response to blue light, plant-type secondary cell wall biogenesis, photosynthesis, light reaction, and photosynthesis, light harvesting, among others (Fig.17B). The differential metabolic pathways between T1S and CKS were mainly enriched in terpenoid biosynthetic process, transferase activity, transferring alkyl or aryl (other than methyl) groups, lactone biosynthetic process, regulation of jasmonic acid mediated signaling pathway, chitinase activity, jasmonic acid metabolic process, phenylpropanoid catabolic process, geraniol 10-hydroxylase activity, and proanthocyanidin biosynthetic process, among others (Fig.17C); between T2S and CKS, the differential metabolic pathways were mainly enriched in abscisic acid binding, isoprenoid binding, lignin catabolic process, phenylpropanoid catabolic process, hormone binding, phenol-containing compound biosynthetic process, proanthocyanidin biosynthetic process, ether metabolic process, and organic acid binding, among others (Fig.17D).

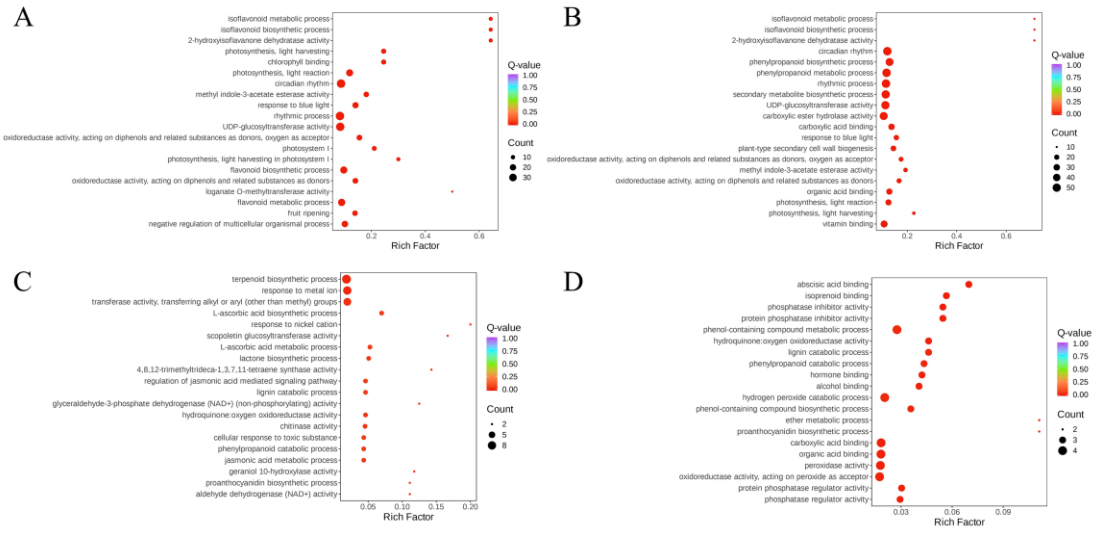

Fig.17 GO enrichment pathways of differentially expressed genes in tea plant leaves (AB) and new shoots (CD) under the influence of ZnO NPs. Enrichment analysis between CKL and T1L

(A); between CKL and T2L (B); between CKS and T1S (C); between CKS and T2S (D). The pathways displayed in the figure all have a Q-value less than 0.05, where Q represents the p-value after correction for multiple hypothesis testing.

qRT-PCR Analysis

To validate the accuracy of the RNASeq data, we randomly selected 20 differentially expressed genes (DEGs), including those related to photosynthesis, sucrose metabolism, and hormones, and verified them using the qRT-PCR method. The expression data of these DEGs from qRT-PCR and RNA-seq are represented by line charts and bar graphs, respectively (Fig.18). The results showed that the expression trends of the genes were highly correlated with the RNA-Seq results, and their patterns of change were essentially consistent. These findings confirm the reproducibility and reliability of the transcriptome data in this study.

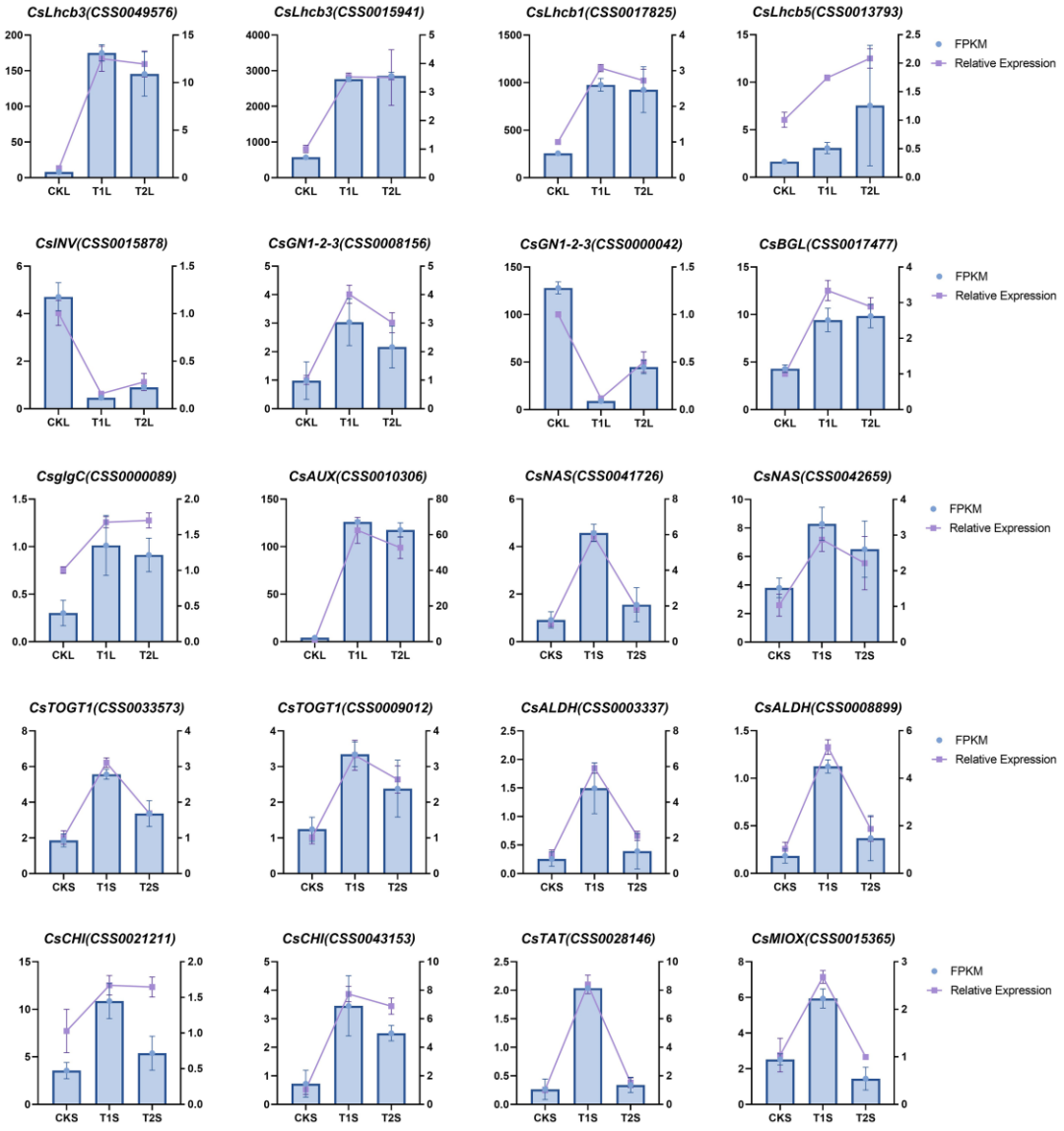

107

108 Fig.18 qRT-PCR validation of 20 DEGs in tea plant leaves and new shoots under the influence of

109 ZnO NPs. The Relative Expression and FPKM of these DEGs are represented by line charts and bar

110 graphs, respectively.

111

112 **Changes in Metabolite Composition and Content in Tea Plant Leaves and New**

113 **Shoots Under the Influence of ZnO NPs**

114 In this study, we conducted a comprehensive targeted metabolomics analysis of tea plants treated

with ZnO NPs using UPLC-MS/MS. A total of 2177 metabolites were detected in the leaves, and 2181 metabolites were detected in the new shoots. Principal component analysis (PCA) showed that in the leaves, PC1 accounted for 26.86% and PC2 accounted for 18.94% of the metabolite variance (Fig.19A); in the new shoots, PC1 accounted for 20.79% and PC2 accounted for 15.64% (Fig.19B). The criteria for selecting differential metabolites in this experiment were based on a Variable Importance in Projection (VIP) > 1 from the OPLS-DA model, along with a fold change ⩾ 2 or fold change ⩽ 0.5. Between T1L and CKL, 179 differential metabolites were detected, with 92 upregulated and 87 downregulated (Fig.20A); between T2L and CKL, 175 differential metabolites were detected, with 99 upregulated and 76 downregulated (Fig.20B). Between T1S and CKS, 83 differential metabolites were detected, with 38 upregulated and 45 downregulated (Fig.20C); between T2S and CKS, 96 differential metabolites were detected, with 48 upregulated and 48 downregulated (Fig.20D). Based on the trend of metabolite concentration changes after treatment with different concentrations of ZnO NPs, the metabolites in tea plant leaves were divided into 8 clusters (Sub class1 had 28, Sub class2 had 37, Sub class3 had 33, Sub class4 had 39, Sub class5 had 38, Sub class6 had 58, Sub class7 had 27, Sub class8 had 58) (Fig.21A); the metabolites in tea plant new shoots were divided into 7 clusters (Sub class1 had 25, Sub class2 had 30, Sub class3 had 14, Sub class4 had 20, Sub class5 had 30, Sub class6 had 26, Sub class7 had 17) (Fig.21B).

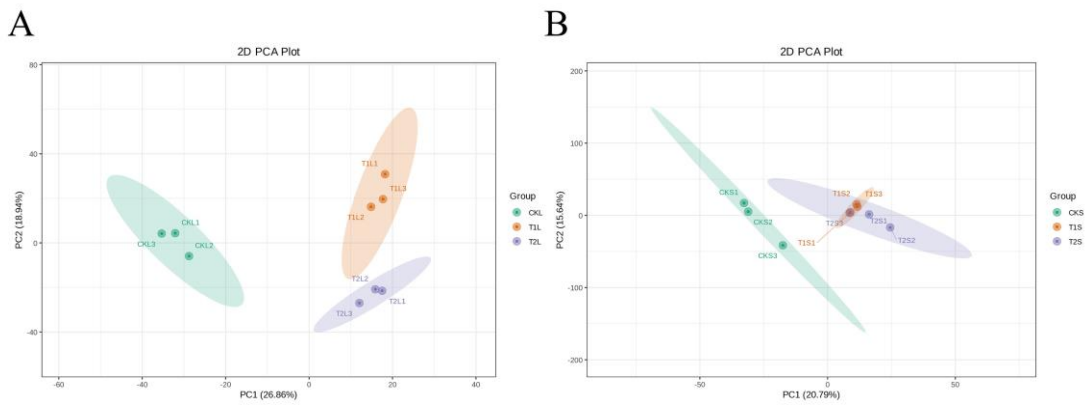

Fig.19 Principal component analysis (PCA) of the comprehensive targeted metabolome in tea plant leaves (A) and new shoots (B) under the influence of ZnO NPs.

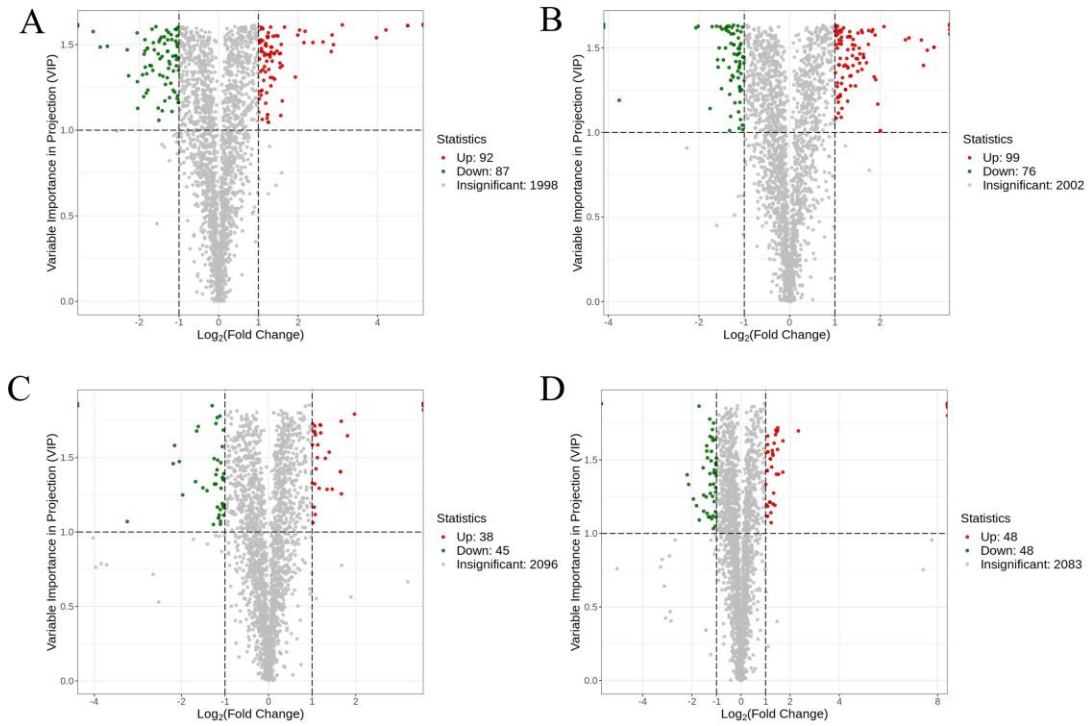

Fig.20 Volcano plots of differential metabolites in tea plant leaves (AB) and new shoots (CD) under the influence of ZnO NPs.

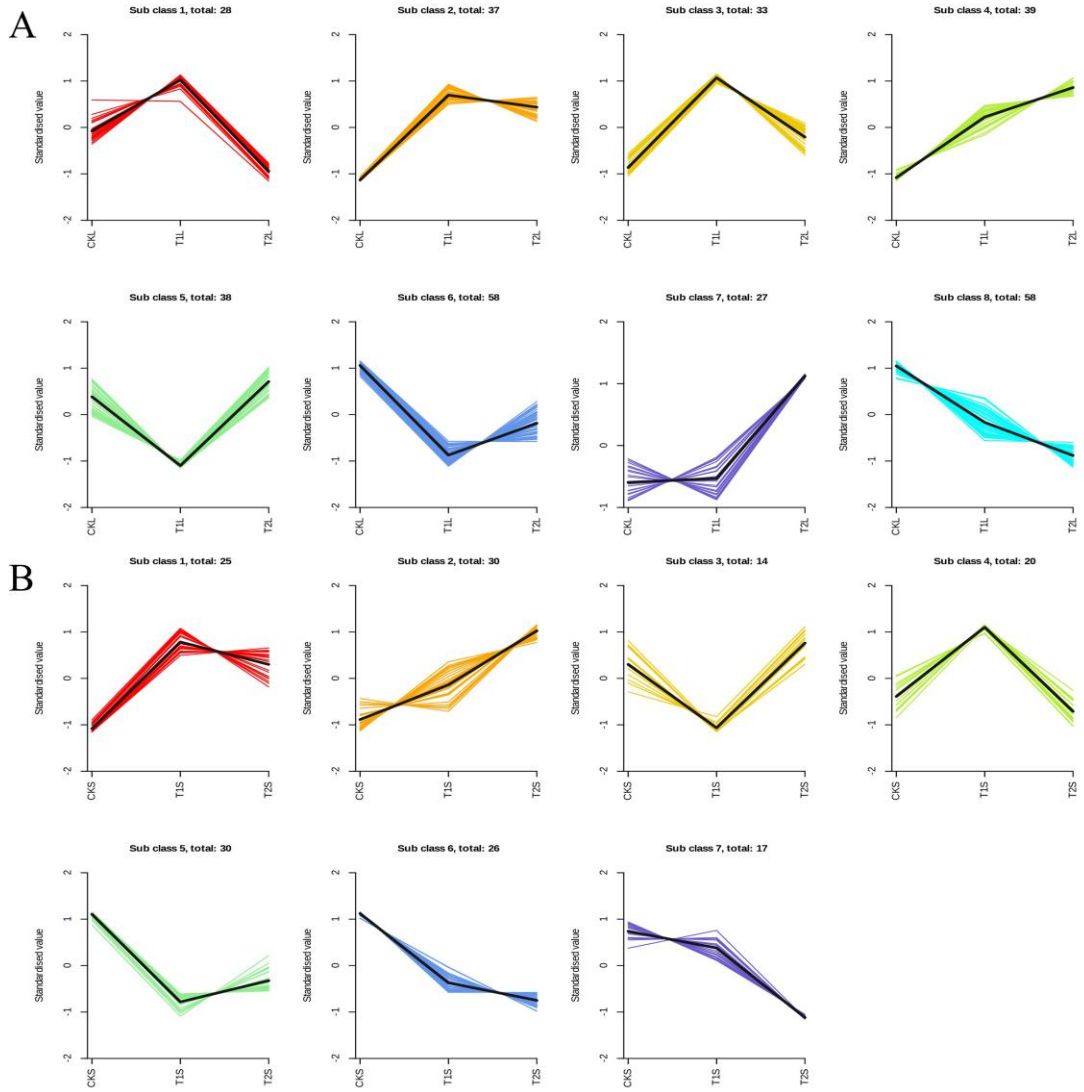

Fig.21 K-means clustering diagrams of differential metabolites in tea plant leaves (A) and new shoots (B) under the influence of ZnO NPs.

Differential Metabolites in Tea Plant Leaves and New Shoots

To cluster and classify samples in the metabolome to reveal similarities and differences between them, we performed a clustering analysis of the samples. As shown in Fig.22, samples within the same group clustered into the same cluster, while samples from different groups clustered into different clusters, indicating good clustering of the samples.

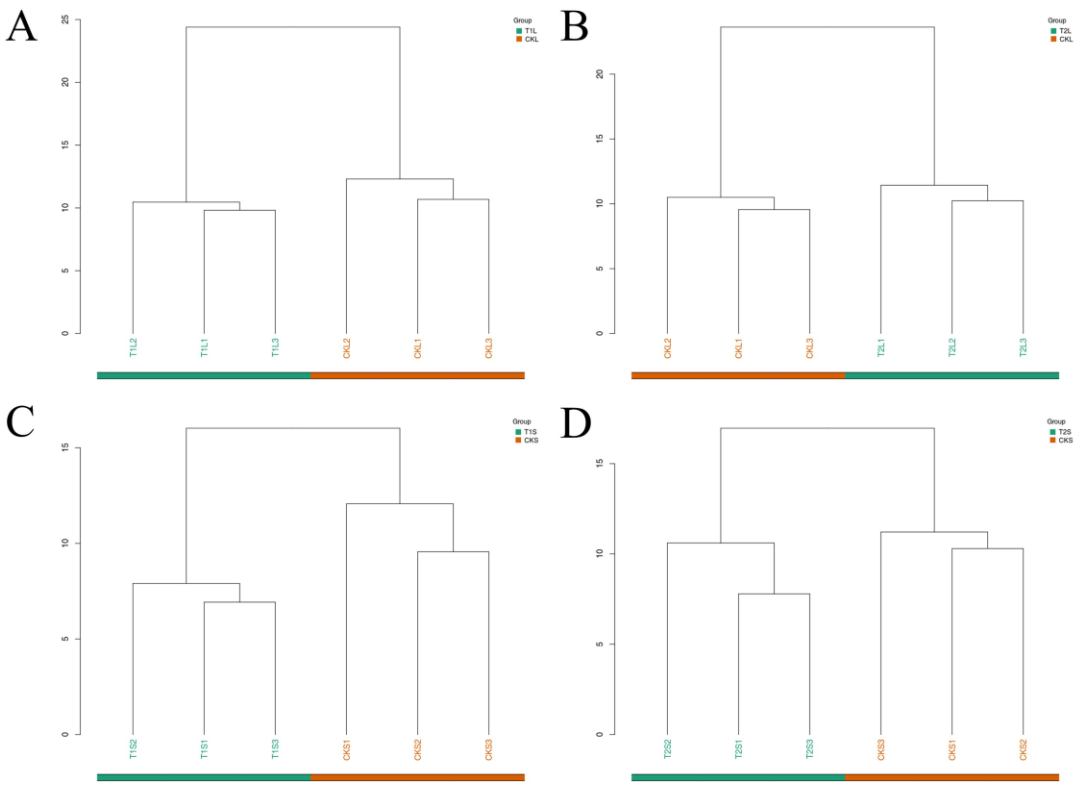

147

148 **Fig.22 Clustering analysis of differential metabolites in tea plant leaves (AB) and new shoots**

149 **(CD) under the influence of ZnO NPs.**

150

151 To elucidate the differences in types and content of metabolites in tea plant leaves and new shoots

152 after ZnO NPs treatment, we selected metabolites with VIP > 1 and FC (fold change) ⩾2 or ⩽0.5

153 as differential metabolites. The results are shown in Fig.23. Fig.23 only displays the top 20

154 metabolites with the highest fold changes in each comparison group, while all differential

155 metabolites between groups are listed in Table.S4 (leaves) and Table.S5 (new shoots). The top 20

156 most significant differential metabolites between T1L and CKL (12 increased and 8 decreased)

157 include Theaflavin-3-gallate, Theaflavin-3'-Gallate, Apigenin-4'-O-(2''-O-p-coumaroyl)-β-D-

158 glucopyranoside, Theaflavin-3,3'-di-O-gallate, Theaflavin, Pinocembrin-7-O-sophoroside, L-

159 Glutamine-O-glycoside, 7-O-(4''-O-glucosyl)coumaroyl-loganic acid, Uridine 5'-diphosphate,

Epitheaflagallin-3-O-Gallate, Prodelphinidin A2 3'-gallate, 4-O-p-Coumaroylquinic acid, Benzoylmalic acid, Rhamnazine-5-O-β-D-glucoside, 3-Cinnamoyl-5-Caffeoylquinic acid, N-Acetyl-L-glycine, Jasmonoyl-L-Isoleucine, LysoPC 19:0, Centaurein, 3,4-Di-O-p-Coumaroylquinic acid (Fig.23A); the top 20 most significant differential metabolites between T2L and CKL (16 increased and 4 decreased) include Theaflavin-3-gallate, Theaflavin-3'-Gallate, 7-O-(4"-O-glucosyl)coumaroyl-loganic acid, Theaflavin-3,3'-di-O-gallate, Apigenin-4'-O-(2"-O-p-coumaroyl)-β-D-glucopyranoside, Theaflavin, Uridine 5'-diphosphate, L-α-Glutamyl-L-Glutamic Acid, Quercetagetin-7-O-glucoside(Quercetagitrin), Gossypetin-3-O-glucoside, Pinocembrin-7-O-sophoroside, 3-O-Galloylepiafzelechin-(4beta->6)-Epigallocatechin-3-O-Gallate, Lys-Asp, Met-Asn, Argininosuccinic acid, 2,6-Dimethyl-6-hydroxy-2,7-octadienyl-β-D-glucoside (Betulalbuside A; Betulabuside A), Benzoylisogomisin O, 6-Deoxyfagomine, Piperidine, Dehydrodiconiferyl alcohol-gamma'-O-glucoside (Fig.23B). The top 20 most significant differential metabolites between T1S and CKS (10 increased and 10 decreased) include 2-[(1R,2R)-3-oxo-2-[(Z)-5-[3,4,5-trihydroxy-6-(hydroxymethyl)oxan-2-yl]oxypent-2-enyl]cyclopentyl]acetic acid, Dicaffeoylquinic acid-O-glucoside, 4'-O-Methyl-6-hydroxygallocatechin 3-O-(N-Ethylglutamine ester) 3'-Gallate, L-Carnitine, Theaflavin-3-gallate, Theaflavin-3'-Gallate, 3-Ureidopropionic Acid, Bletilols B, Tricin-7-O-(4'-O-glucoside)-guaiacylglycerol-ether, Pinoresinol-4,4'-O-diglucoside, LysoPC 20:4, 1-O-Feruloylquinic acid, Planteose, 8R-Dihydrodehydrodiconferyl alcohol 4-O-β-D-glucopyranoside, 1,4,8-Trihydroxynaphthalene-1-O-[6'-O-(3",4",5"-trimethylbenzoyl)]glucoside, Luteolin-5,7-di-O-rutinoside, 1-(4-Hydroxybenzoyl)Glucose; 25545-07-7, Phenyl acetate, Glucan, Theasinensin F (Fig.23C); the top 20 most significant differential metabolites between T2S and CKS (10 increased and 10 decreased) include Dicaffeoylquinic acid-O-glucoside, Pinocembrin-7-

O-sophoroside, Adenylocuccinic Acid, L-Carnitine, Theaflavin-3,3'-di-O-gallate, Apigenin-4'-O-(2"-O-p-coumaroyl)-β-D-glucopyranoside, Fagomine, 2,3-O-(S)-hexahydroxydiphenoyl-D-glucose, Sinapoyl malate, Theaflavin, Punigluconin, 1,4,8-Trihydroxynaphthalene-1-O-[6'-O-(3",4",5"-trimethylbenzoyl)]glucoside, 1-Methoxybenzoyl-6-O-Galloyl-D-Glucose, Juglanin, D-Glucosamine, Dehydrodiconiferyl alcohol-gamma'-O-glucoside, Ethyl 3-hydroxybutyrate, Methyl 3-(3-hydroxy-4-methoxyphenyl)propanoate, 3,3'-O-Dimethylellagic Acid-4'-O-arabinoside, Theasinensin F (Fig.23D).

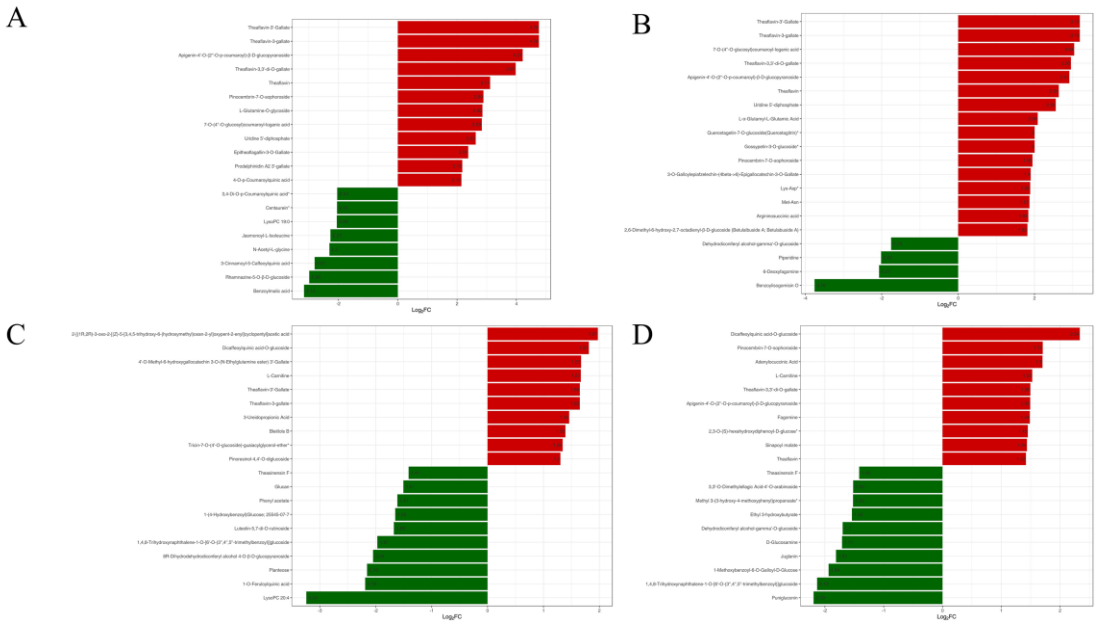

Fig.23 The top 20 metabolites with the greatest difference in tea plant leaves (AB) and new shoots (CD) under the influence of ZnO NPs. Differential metabolites between CKL and T1L (A); between CKL and T2L (B); between CKS and T1S (C); between CKS and T2S (D). The colors in the figure indicate an increase (red) or decrease (green) in content.

KEGG Enrichment Analysis of Differential Metabolites

To study the impact of ZnO NPs on the metabolic pathways in tea plants, we performed KEGG

197 enrichment analysis on the differential metabolites in leaves and new shoots treated with ZnO NPs.
198 The results are shown in Fig.24. The differential metabolic pathways between T1L and CKL were
199 mainly enriched in Starch and sucrose metabolism (ko00500, p=0.002), Linoleic acid metabolism
200 (ko00591, p=0.014), Arginine biosynthesis (ko00220, p=0.02), Anthocyanin biosynthesis (ko00942,
201 p=0.031), Betalain biosynthesis (ko00965, p=0.031), Biotin metabolism (ko00780, p=0.031),
202 Aminoacyl-tRNA biosynthesis (ko00970, p=0.037), Galactose metabolism (ko00052, p=0.037),
203 Caffeine metabolism (ko00232, p=0.0415); the differential metabolic pathways between T2L and
204 CKL were mainly enriched in Starch and sucrose metabolism (ko00500, p=0.002), Carbon fixation
205 in photosynthetic organisms (ko00710, p=0.010), Glucosinolate biosynthesis (ko00966, p=0.010),
206 Tropane, piperidine and pyridine alkaloid biosynthesis (ko00960, p=0.010), Metabolic pathways
207 (ko01100, p=0.012), Biosynthesis of amino acids (ko01230, p=0.013), 2-Oxocarboxylic acid
208 metabolism (ko01210, p=0.014), Aminoacyl-tRNA biosynthesis (ko00970, p=0.0154), Betalain
209 biosynthesis (ko00965, p=0.041), Cyanoamino acid metabolism (ko00460, p=0.043). The
210 differential metabolic pathways between T1S and CKS were mainly enriched in Pantothenate and
211 CoA biosynthesis (ko00770, p=0.019), One carbon pool by folate (ko00670, p=0.021), beta-Alanine
212 metabolism (ko00410, p=0.023); the differential metabolic pathways between

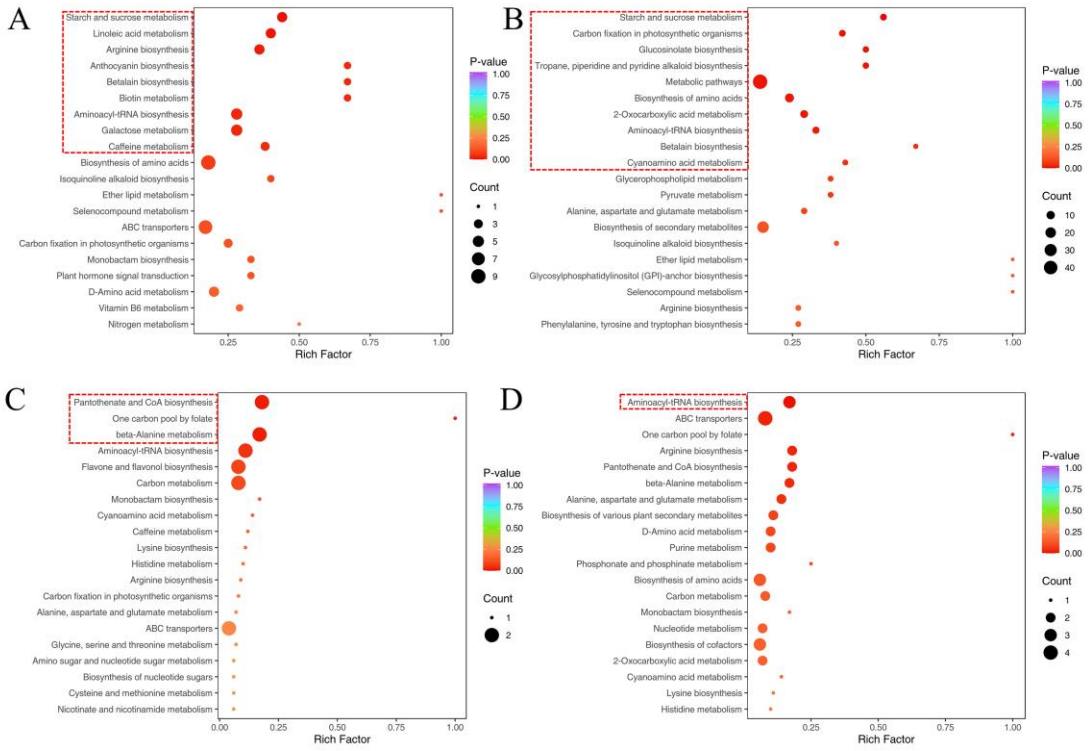

Fig.24 KEGG enrichment pathways of differential metabolites in tea plant leaves (AB) and new shoots (CD) under the influence of ZnO NPs. Enrichment analysis between CKL and T1L (A); between CKL and T2L (B); between CKS and T1S (C); between CKS and T2S (D). Pathways within the red dashed box have a p-value < 0.05.